Heterodimer Formation and Crystal Nucleation of Gramicidin D

Brian M. Burkhart, Ryan M. Gassman, David A. Langs, Walter A. Pangborn, and William L. Duax
Hauptman-Woodward Medical Research Institute, Inc., Buffalo, New York 14203-1196 USA

ABSTRACT The linear pentadecapeptide antibiotic gramicidin D is a heterogeneous mixture of six components. Precise refinements of three-dimensional structures of naturally occurring gramicidin D in crystals obtained from methanol, ethanol, and n-propanol demonstrate the unexpected presence of stable left-handed antiparallel double-helical heterodimers that vary with the crystallization solvent. The side chains of Trp residues in the three structures exhibit sequence-specific patterns of conformational preference. Tyr substitution for Trp at position 11 appears to favor β ribbon formation and stabilization of the antiparallel double helix that acts as a template for gramicidin folding and nucleation of different crystal forms. The fact that a minor component in a heterogeneous mixture influences aggregation and crystal nucleation has potential applications to other systems in which anomalous behavior is exhibited by aggregation of apparently homogeneous materials, such as the enigmatic behavior of prion proteins.

INTRODUCTION

Linear gramicidin, a pentadecapeptide antibiotic isolated from *Bacillus brevis* (Dubos, 1939) is active against Gram-positive bacteria (Hotchkiss, 1944; Gross and Witkop, 1965) by forming membrane channels that are specific for monovalent cations (Pressman, 1965). The antibiotic consists of alternating D- and L-amino acids in the sequence HCO-L-Val_1-Gly_2-L-Ala_3-D-Leu_4-L-Ala_5-D-Val_6-L-Val_7-D-Val_8-L-Trp_9-D-Leu_{10}-L-Trp_{11}-D-Leu_{12}-L-Trp_{13}-D-Leu_{14}-L-Trp_{15}-$NHCH_2CH_2OH$ (Sarges and Witkop, 1965). Naturally occurring gramicidin is a mixture of isoforms differing in amino acid composition at position 1, Val_1 (Vg)/Ile_1(Ig), and position 11, Trp_{11}(gA)/Phe_{11}(gB)/Tyr_{11}(gC) (Sarges and Witkop, 1965). Electrophysiological measurements indicate that several types of channels having different conductance levels, channel accumulation, and duration of channel opening are observed for homo and heterodimers of natural and synthetic gramicidin and their mixtures (O'Connell et al., 1990; Sawyer et al., 1989; Oiki et al., 1994; Koeppe et al., 1985, 1991, 1992, 1995). Numerous models have been proposed for the structure of gramicidin in various solvents and in lipid bilayers (Urry, 1971; Veatch and Stryer, 1977; Arseniev et al., 1992; Ketchem et al., 1993; Stark et al., 1986; Pascal and Cross, 1993; Bouchard et al., 1995; Cotten, 1997). Although it appears that the conducting form of the molecule is most probably a dimer (Veatch and Stryer, 1977), there is evidence that several types of dimers, including a head-to-head single-stranded form (Urry, 1971), left- and right-handed double-stranded parallel and antiparallel helical forms (Veatch and Stryer, 1977), and a possible tetrameric form (Stark et al., 1986) exist and may have some functional role. It has been proposed that tryptophan conformations and conformational changes are specifically correlated with gramicidin orientation in and association with membrane lipids, ion coordination, and bilayer ion transport (Salom et al., 1995; Becker et al., 1991; Takeuchi et al., 1990; Seoh and Busath, 1995; Woolf and Roux, 1997; Jing and Urry, 1995; Roux and Woolf, 1997; Urry et al., 1982a; Nekrasov et al., 1995; Separovic et al., 1994; Smith et al., 1990; Roux et al., 1995). The tryptophan residues at the four sites [In the structures, the two strands are designated as 101–116 and 201–216. If a general description of residues is indicated in the text, then the numbering will be 1–16] (9, 11, 13, and 15) differ significantly with respect to these properties (Becker et al., 1991). Studies of naturally occurring and synthetic isomers indicate that amino acid variation at position 11, in particular, has significant effects on channel opening, duration, and transport properties (Becker et al., 1991).

A left-handed antiparallel β-helix conformation (Fig. 1) has been found in crystals of uncomplexed gramicidin, obtained from methanol (Langs et al., 1991), ethanol (Langs, 1988), and n-propanol (this report), and in gramicidin complexes with KSCN (Doyle and Wallace, 1997) and CsCl (Wallace and Ravikumar, 1988). NMR studies of gramicidin in benzene/ethanol and of a gramicidin Cs^+ complex in methanol (Nekrasov et al., 1995) predict Trp conformations similar to those observed in crystals obtained from ethanol and n-propanol. We have recently determined the structure of a crystal form prepared from n-propanol and completed the full-matrix restrained anisotropic refinements of all atomic positions in gramicidin in all three crystal forms of gramicidin D.

MATERIALS AND METHODS

Crystals of gramicidin D were grown from a heated 30 mg/ml solution in n-propanol containing 2% (w/v) PEG 4000. Although individual batches of gramicidin D differ in composition, the material used to prepare the crystals came from Sigma Chemical Company (St. Louis, MO) and was

Received for publication 24 November 1997 and in final form 10 August 1998.

Address reprint requests to Dr. William L. Duax, Hauptman-Woodward Medical Research Institute, Inc., 73 High Street, Buffalo, New York l4203-1196. Tel.: 716-856-9600; Fax: 716-852-6086; E-mail: duax@hwi.buffalo.edu.

0006-3495/98/11/2135/12 $2.00

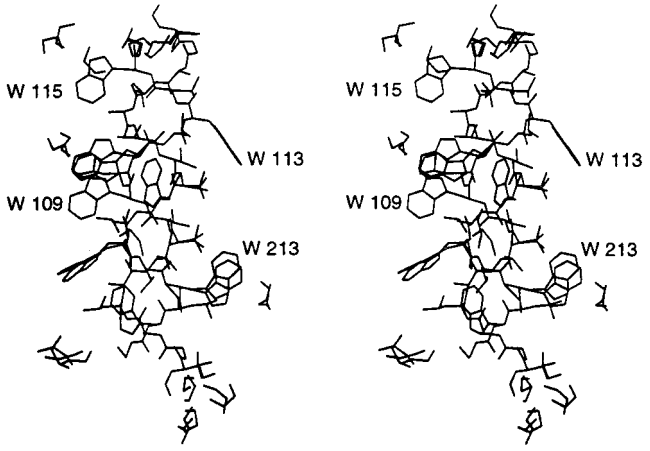

FIGURE 1 Stereo illustration of the antiparallel β-helical forms of gramicidin D observed in crystals obtained from n-propanol. Disordered Trp's and disordered n-propanol molecules, including those hydrogen-bonded to three of the Trp (W-9, W-15, and W-13) residues, are shown. All figures of molecular structures were drawn using the program CHAIN (Sack, 1988).

labeled 80% gA, 6% gB, 14% gC, and an unspecified percentage of Ig. HPLC separation of the sample of the starting material produced peaks corresponding to gC and gA with a satellite that would correspond to IgG and IgA, but no unequivocal signal for gB (data not shown). Single crystals appeared in approximately one month and grew to an approximate size of $0.3 \times 0.3 \times 0.7$ mm. During data collection, the diffracting crystal was mounted inside a fiber loop (Hampton Research, Laguna Niguel, CA) and flash-frozen with liquid nitrogen with the n-propanol/PEG mother liquor acting as its own cryoprotectant. The crystals diffracted to the limit of the RAXIS II image plate detector using CuKα radiation and a full data set was collected to 1.13 Å. The cell constants of the unit cell were determined to be a = 32.434 Å, b = 32.461 Å, and c = 24.148 Å in space group $P2_12_12_1$. A total of 67561 observations were recorded of which 9572 were unique with an R_{merge} of 4.1%. The highest resolution shell (1.16–1.13 Å) had an R_{merge} of 6.5% and an $\langle I/\sigma I\rangle$ of 13.0.

Because the n-propanol unit cell was approximately isomorphous to the ethanol solvate of gramicidin (Langs, 1988), the coordinates from the refined structure (see below), stripped of all solvent and disordered components, was refined against F^2 using SHELXL-97 (Sheldrick, 1997). Disordered components and n-propanol solvents were identified with difference (F_o-F_c) electron density maps and modeled if they made chemical sense, with monitoring during refinement using R_{free} (Brunger, 1992). Re-refinements of the methanol and ethanol solvates were performed in the same manner using their original data sets. The refined coordinates have been deposited in the PDB (Bernstein et al., 1977) with reference codes 1ALX (methanol), 1ALZ (ethanol), and 1AL4 (n-propanol).

RESULTS

As a result of the high quality of the low temperature data used in the refinements and the use of restrained anisotropic thermal parameter refinement, we have been able to determine for the first time that significant amounts of ordered heterodimers are present in each crystal form, in addition to the expected homodimers. The heterodimers of VgA/VgC were identified by detection of an ordered Tyr_{11} side chain on only one strand of the dimer. The presence of the residue was detected in difference electron density maps calculated during the late stages of the refinements (Fig. 2). The

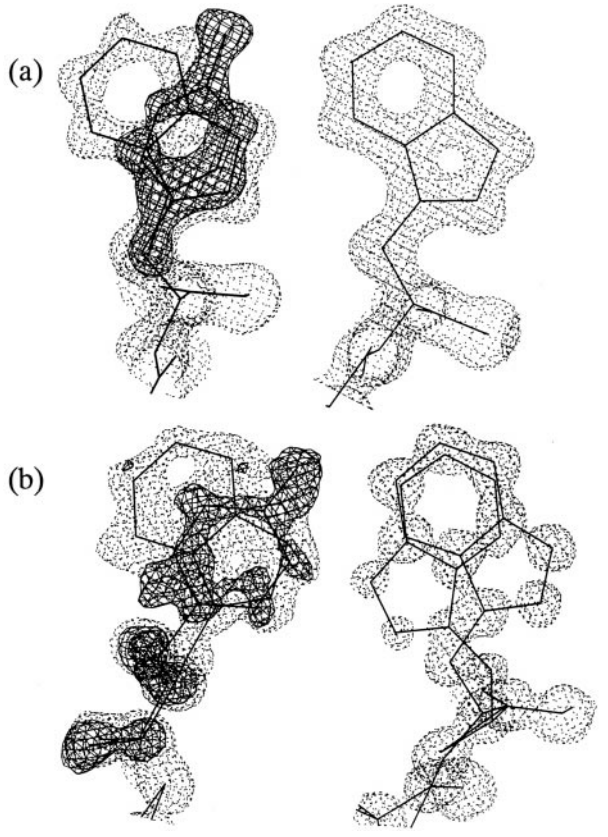

FIGURE 2 2-F_o-F_c electron density maps (*stippled*) and F_o-F_c difference maps (*solid mesh*) reveal the presence of 20–30% occupancy by tyrosine residues at position 111 on only one strand of the β-helical dimer in both the monoclinic crystal form obtained from methanol (*a*) and the orthorhombic form obtained from ethanol (*b*). For the calculations the Tyr_{111} side chains were omitted and the Trp_{111} residues were included at 0.70 occupancy. The difference density was contoured at 3σ. The 2-F_o-F_c electron density map is superimposed and contoured at 1σ. The 100% occupancy Trp_{211}, ordered in methanol (*a*) and 50/50 disorder in ethanol (*b*), are shown for comparison.

refined group occupancy for the Tyr_{11} side chain relative to the Trp_{11} side chain is 31%/69% in crystals obtained from ethanol and 25%/75% in crystals obtained from methanol. HPLC separation of gramicidin from dissolved crystals obtained from methanol and ethanol reveal the presence of a mixture of gA and gC. The introduction of a partial occupancy Tyr in these ratios during refinement resulted in reduction in the *R* factor of 0.4% and 0.8% in the methanol and ethanol structure, respectively; a significant reduction for the addition of a few partial atoms. Thermal parameters for both Trp_{11} and Tyr_{11} are similar in each crystal structure, suggesting that the occupancy is not skewed by changes in the thermal parameters of the relevant atoms. We found no evidence of Ile_1 in the single crystals grown from methanol. However, in crystals grown from n-propanol, Ile_1 residues are found on both strands of the double helix and the occupancy is ~20% at each site. This may be due to random distribution of Ile_1 substituted strands among homo and heterodimers or disordered crystallization of VgA/IgA heterodimers. We found no evidence of Tyr_{11} in the crystals

TABLE 1 Gramicidin D crystal and refinement data

	Methanol	Ethanol	n-Propanol
Crystal System	Monoclinic	Orthorhombic	Orthorhombic
Space Groups	$P2_1$	$P2_12_12_1$	$P2_12_12_1$
Cell Constants	a = 14.907 Å b = 26.014 Å c = 31.911 Å $\alpha = \gamma = 90.0°$ $\beta = 92.1°$	a = 31.595 Å b = 32.369 Å c = 24.219 Å $\alpha = \beta = \gamma = 90.00$	a = 32.434 Å b = 32.461 Å c = 24.148 Å $\alpha = \beta = \gamma = 90°$
Resolution	1.20 Å	0.86 Å	1.13 Å
Number of data [$F > 4\ \sigma\ (F)$]	7726 [7726]	21,454 [10,782]	9571 [9165]
$R(F)$ [$R(F > 4\ \sigma(F))$]*	8.91% [8.91%]	16.41% [11.03%]	6.71% [6.58%]
Number of Parameters	3094	3489	3788
Number of Restraints	5995	7373	7555
Observation/Parameters	4.4 [4.4]	8.3 [5.2]	4.5 [4.4]

*The reflection weighting scheme used is Weight = $[\sigma^2(F_o^2) + (0.2P)^2]^{-1}$ where P = 1/3 [max(0, F_o^2) + $2F_c^2$].

grown from n-propanol and no evidence of Phe_{11} in crystals from any of the three solvents. The crystal and refinement data for the three structure determinations are presented in Table 1. The average temperature factors are given in Table 2. The RMSD values for the bond length average 0.014 Å in the methanol complex and 0.016 Å in the ethanol and propanol structures.

All three structures are left-handed antiparallel double helixes with ~5.6 residues/turn. Since the n-propanol and ethanol structures have isomorphous cell constants, the structures are very similar to one another. The methanol structure differs from the other two in that most Trp residues are oriented with their planes parallel to the helix axis and their ring nitrogens hydrogen-bonded to methanol molecules. The Trp residues in the ethanol and n-propanol are oriented with their planes approximately perpendicular to the helix axes, and few of them are associated with solvent. When the six crystallographically independent backbones are superimposed by least-squares fit of the first five Cα carbons (Fig. 3), one strand of the six appears to be distinctly different. This is the Tyr-containing strand in the dimer grown from methanol.

The methanol structure contains several discretely disordered residues: Val_{107} (82/18), Val_{206} (72/28), Val_{208} (70/30), and Leu_{210} (44/56). The ratios of occupancy are shown in parentheses. In addition, both ethanolamine residues, EAM_{116} (45/25/30) and EAM_{216} (41/30/29), occur in three orientations. In the ethanol structure, only four side chains are discretely disordered: Leu_{112} (70/30), Leu_{210} (75/25), Trp_{211} (58/42), and Trp_{213} (42/58). This disorder is highly correlated, with neighboring Trp_{211}/Trp_{213} residues from symmetry-related dimers interacting, which appears to contribute to disorder in the nearby Leu_{112} and Leu_{210}. The ethanolamines are fully ordered and form hydrogen bonds to the backbone with the same dimer via end-to-end interactions between translationally related dimers. The n-propanol structure is isomorphous to the ethanol structure with a slight expansion along the *a* axis. There are five disordered side chains: Val_{107} (89/11), Trp_{111} (60/40), Val_{208} (78/22), Trp_{211} (70/30), and Trp_{213} (61/39). One of the two ethanolamines, EAM_{116} (45/2936/19), is threefold disordered. There is no evidence for Tyr at either 11 position, although this could be masked by the disorder at each site. Nearly all of the solvents are disordered, to some extent, in all three crystal forms. However, solvent does seem to play a key role in gramicidin side chain conformation and in selecting the composition of gramicidin in the crystals. Details of the solvent structure are presented in Table 3.

TABLE 2 Average temperature factor of the peptide backbone atoms, side chain action, and solvent in the three crystal structures

Structure	⟨B⟩ Peptide Backbone	⟨B⟩ Side Chain	⟨B⟩ Solvent
Methanol	6.6Å^2	8.8Å^2	18.1Å^2
Ethanol	5.3Å^2	8.1Å^2	14.5Å^2
n-Propanol	7.9Å^2	10.3Å^2	16.3Å^2

The gramicidin dimers are linked together to form infinite chains running approximately parallel to one another in each of the three crystal structures. These infinite chains are stabilized by hydrogen bonding between the N-termini of translationally related dimers. The alignment of the adjacent dimers and solvent interactions at the interface between them differs in the three structures. The hydrogen bonds linking the dimers together are strongest in the methanol complex and weakest in the n-propanol complex (Fig. 4). In the ethanol and n-propanol complexes, an alcohol molecule competes for the hydrogen bond to the formyl group so that the formyl carbonyl to the Leu_4 NH distance increases from 2.80 Å to 3.80 Å to 4.05 Å as the solvent changes from methanol to ethanol to n-propanol.

The principal difference between the monoclinic (methanol) and orthorhombic (ethanol and n-propanol) crystal forms concerns the position of the infinite chains relative to each other. The tyrosine present in only 25–30% of the heterodimers appears to influence the registry of adjacent chains in crystals grown from methanol and ethanol. Adjacent gramicidin chains in crystals grown from ethanol are connected by a sequence of hydrogen bonds involving a

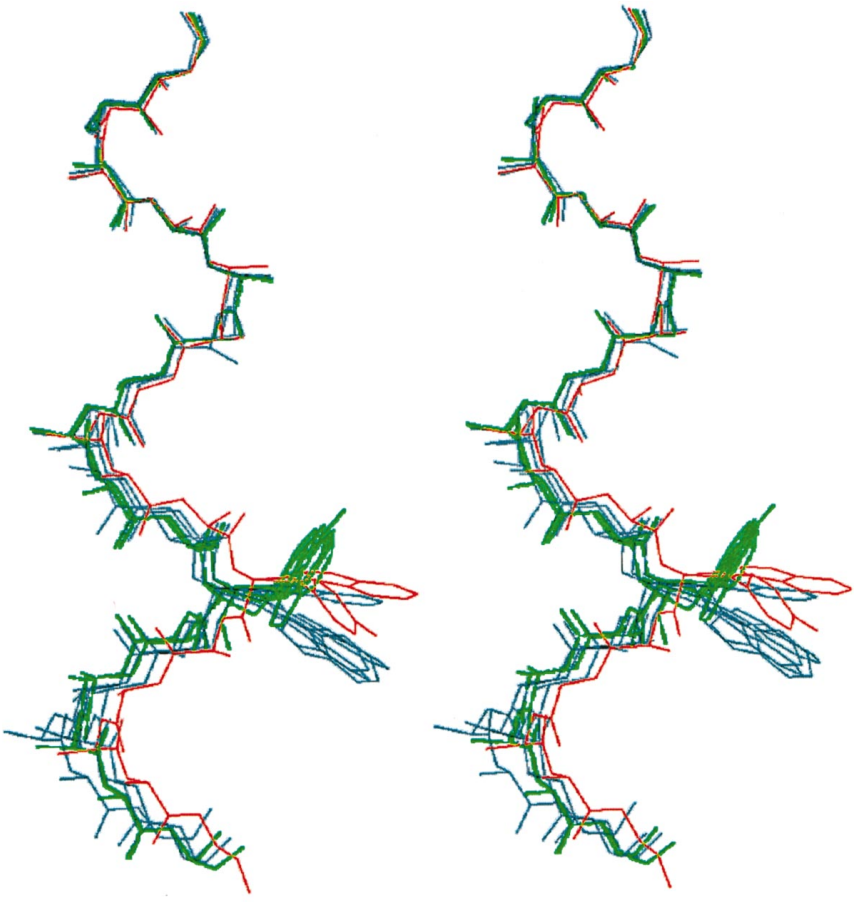

FIGURE 3 Least-squares-fit of the backbone atoms of the first five residues in the six crystallographically independent monomers in the structures crystallized from methanol (M1 and M2), ethanol (E1 and E2), and n-propanol (P1 and P2) reveal that P1 and E1 (*green*) have nearly identical conformations, P2 and E2 (*blue*) have nearly identical conformations and diverge from P1/E1 at residue 11, M2 (also *blue*) is much like P2/E2 but diverges from them at Leu_{12}, and M1 (*red*) deviates most from all others, diverging from M2 at Val_8.

water molecule and an ethanol molecule that link a Tyr_{11} hydroxyl on one chain to a Trp_{15} carbonyl oxygen of another (Fig. 5 *a*). These hydrogen-bonded Tyr and ethanol molecules link adjacent chains like the rungs in a ladder. The infinite chains linked by the Tyr/ethanol rungs are related to one another by a crystallographic screw axis parallel to the axis of the tubes, as illustrated in Fig. 5 *b*. The packing of adjacent chains in crystals grown from n-propanol is nearly identical to that in the ethanol complex, but no interstrand chains of hydrogen bonded molecules can be detected. Crystals grown from methanol exhibit a more well-defined layered structure than is observed in crystals grown from ethanol and n-propanol. The layers of methanol alternate with layers of gramicidin in which the more hydrophobic surfaces of the gramicidin dimers are packed together. The nitrogens of all Trp residues are hydrogen-bonded to methanol oxygens. The 13 hydrogen bonds range in length from 2.60 to 3.17 Å (avg = 2.92 ± 0.15 Å). The Tyr residues are embedded in the surface of the solvent layers and orient the gramicidin chains relative to them. The alignment of adjacent chains related by rotational symmetry and the alternating layers of gramicidin chains and solvent molecules in the crystal form obtained from methanol are shown in Fig. 6.

TABLE 3 Characteristics of solvent in crystalline complexes

Solvent	Methanol	Ethanol	n-Propanol
Dielectric constant*	32.6	24.3	20.1
Number/unit cell	42	54	44
Sites/unit cell	70	84	88
Bulk solvent g#	0.1279	0.2214	0.5373
Bulk solvent U#	0.8232	1.2947	0.7755

*From CRC Handbook of Chemistry & Physics, 56th Edition (1976).
#F_c^2 (new) = F_c^2 (old) · (1 − g · exp[−8 $\pi^2 U(\sin\theta/\lambda)^2$]).

The observed conformations of the Trp residues were examined to identify any patterns of unusual features of position 11, the site of structural isomerism arising from a mixed population of Tyr, Trp, and Phe residues. To compare observed conformational features of the D, L amino acids in gramicidin with data from the Protein Data Bank (PDB) (Bernstein et al., 1977) the signs of the torsion angles of the D residues have been inverted to correspond to the mirror-image L enantiomers. The ψ, ϕ values for the 15 residues in the three dimers (a total of 90 residues including disorder) are listed in Table 4 and plotted in Fig. 7 *a*, and compared with the distribution observed in well-determined structures taken from the PDB (Kleigwegt and Jones, 1996). All of the amino acid conformations in gramicidin are in the region of the ψ, ϕ plot typical of β-structures. The most significant feature of the distribution is that the Trp residues lie outside the contour that encompasses 95% of all amino acid conformations. Although the ψ, ϕ values for the 11 position on

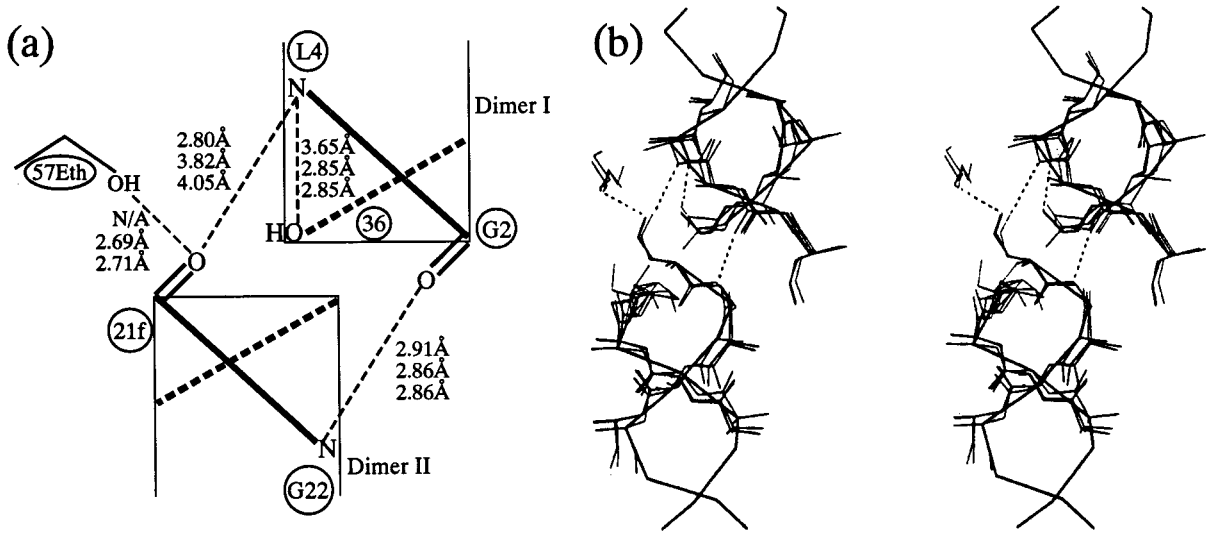

FIGURE 4 (*a*) Schematic of hydrogen bonds connecting two translationally related dimers. Hydrogen bonds link translationally related gramicidin dimers via the N-termini in crystals prepared from methanol, ethanol, and n-propanol (top to bottom). The methanol form contains two hydrogen bonds [(N_4–OF_{21} and (O_2–N_{22})] between Y and W strands in translational related dimers. In the ethanol form OF_{21} is hydrogen-bonded to the ethanol rather than to N_4, and the ethanolamine residue forms a hydrogen bond between OG_{36} and N_4. In the n-propanol form, the interaction between adjacent dimers is further reduced. (*b*) Stereo view of same region.

the Tyr-rich strands of the heterodimer are of necessity an average of values for Trp and Tyr, the ψ, ϕ magnitudes at position 11 in the mixed occupancy strand are closer to the densely populated portion of the β region than the ϕ, ψ values for full occupancy Trp's.

When the χ_1 and χ_2 values (Table 5) for the Trp and Tyr residues are examined (Fig. 7 *b*) the significantly different conformational properties of the amino acid side chains at position 11 emerge. Because of the partial occupancy of the Tyr and Trp residues at position 11 in the heterodimers, the twofold disorder of the Trp_{11} and Trp_{13} in the ethanol complex, and the twofold disorder of Trp_{11} in the propanol complex, there are 29 observed χ_1/χ_2 pairs. In the plot, 24/29 residues have χ_1 values of $\sim$180°. The five exceptions are the four Trp_{11}'s and one Tyr. The majority of the Trp's at positions 9, 13, and 15 of both strands of the two-stranded β-coil (15 of 19) have conformations with $\chi_1 = -166 \pm 13°$ and $\chi_2 = -96 \pm 18°$. Variation of the χ_1 and χ_2 values in this subset is highly correlated (Fig. 7 *d*). None of the Trp_{11} residues fall in this region of conformational space. All eight full and partially occupied Trp_{11} residues on either strand of the hetero and homodimers are in less favored regions of conformational space (Fig. 7, *e* and *f*) and four of them are among the five having χ_1 values closer to $\pm 90°$ than to 180°. In one of these unusual conformations [χ_1, $\chi_2 = -60°, -60°$] the indole ring lies so close to the gramicidin backbone that contacts of less than van der Waals distance are made between the ring and the carbonyl group of Leu_{10} (Fig. 7 *f*). There is ^{13}C-NMR evidence that this carbonyl is the site of ion association in the conducting form of gramicidin. The two Tyr_{11} residues have χ_1 and χ_2 values similar to those of the Trp_{11}. The Trp residues in crystals grown from methanol all have χ_1 values near 180°, but have a much broader range of χ_2 values than do the Trp residues in crystals prepared from ethanol or n-propanol (Fig. 7, *b* and *f*).

There is a correlation between Trp conformations and solvent association in the crystals. Hydrogen bonding between the Trp nitrogen and solvent molecules is observed for seven of eight Trp residues in the methanol complex, but only three of the eight Trp residues in the ethanol and n-propanol complexes. The stereospecific pattern of methanol association with the Trp in the complex (Fig. 8) correlates well with the rotation around the Cα-Cβ bond (χ_2 values) forming the bouquet-like appearance of the Trp's when the Cα-Cβ bonds are superimposed (Fig. 7 *c*). In contrast, in the crystals grown from ethanol and propanol, the Trp side chains do not hydrogen-bond with the solvent. A correlated variation of the Trp χ_1, χ_2 values is observed in the crystal that is in excellent agreement with the conformations found by NMR in uncomplexed gramicidin in benzene/ethanol (Zhang et al., 1992) (Fig. 7 *d*) and the gramicidin CsCl complex in methanol (Nekrasov et al., 1995).

DISCUSSION

The presence of distinct heterodimers in significantly different crystal forms demonstrates that the heterodimers are not an artifact of crystallization. The strongest interactions between adjacent columns of gramicidin dimers in crystals obtained from ethanol are hydrogen bonds involving the Tyr 11 and the ethanol (Fig. 5). This suggests that tyrosine residues of the heterodimers nucleate and define this crystal form. The fact that crystals grown from methanol and eth-

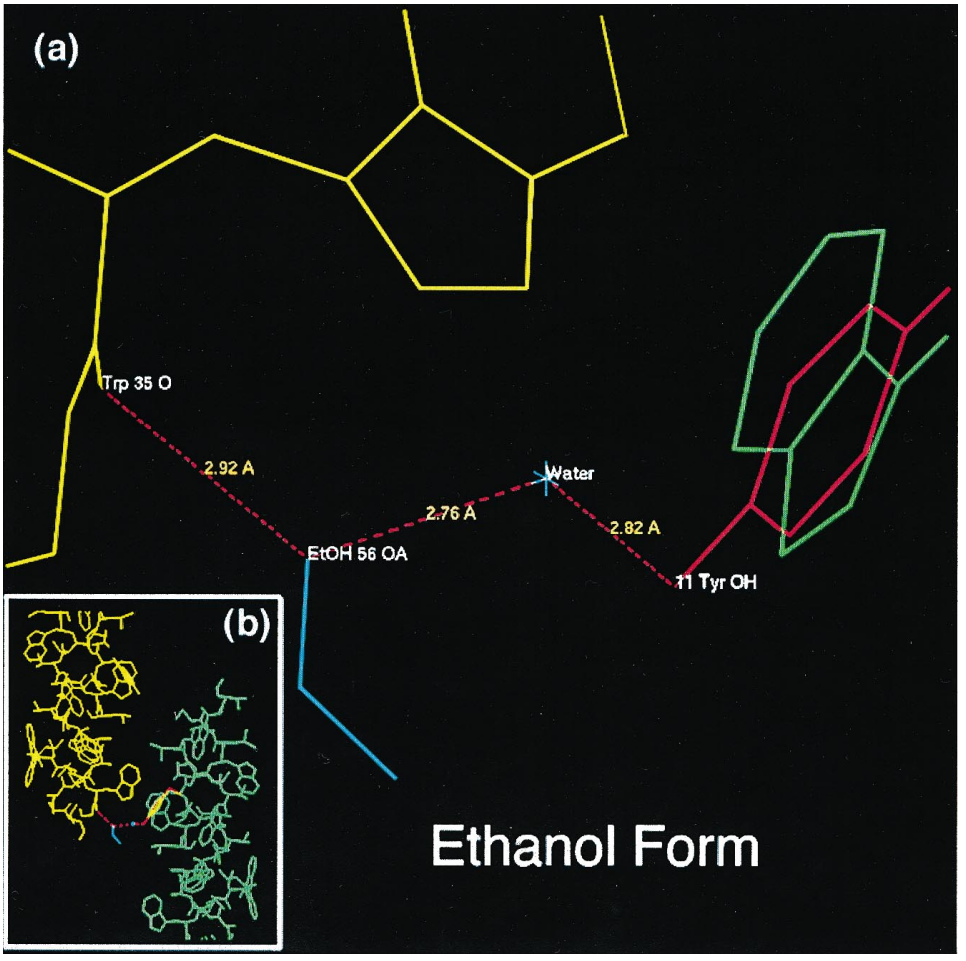

FIGURE 5 The strongest interaction between adjacent infinite chains of β-helical dimers in the ethanol complex involves an ethanol and a water molecule that link the partial occupancy Tyr_{11} to a carbonyl on the backbone of a Trp_{215} residue on an adjacent chain. The Tyr_{111}, ethanol, water, carbonyl sequence is shown in (*a*). (*b*) Illustration of the relative position of the chains linked by this hydrogen bond network to form infinite ladders with tyrosine/water/ethanol rungs.

anol each contain 20–30% heterodimers of gramicidin A and C and 70–80% homodimers of gramicidin A indicate that suitable packing interactions can be satisfied without full occupancy by heterodimers. The presence of gramicidin C in the crystallization media of the propanol complex may be sufficient for nucleation of the antiparallel double-helical crystal form. The fact that single crystals grown from n-propanol solution contain 20% Ile on both strands suggest that homo and heterodimers containing Ile are less soluble in and preferentially precipitate from n-propanol. It is worth noting that the intramolecular interactions in both the methanol and ethanol crystal forms are of sufficient importance to crystallize an ordered heterodimer. If the heterodimers had crystallized in a disordered fashion, conforming to the pseudo-twofold symmetry perpendicular to the helix axis relating the two β-chains, it would have been impossible to detect that the antiparallel β-helix was in fact a heterodimer. For this reason, it is impossible to ascertain whether a disordered arrangement of heterodimers of IgA/VgA is present in crystals grown from n-propanol.

A very tight seamless fit of hydrogen bonds is attributed to the NH_2-terminus to NH_2 terminus dimer that is claimed to be the membrane channel form of gramicidin (Durkin et al., 1986). In all three crystal forms, there are H bonds between the N-termini of translationally related dimers forming what could be loosely termed a "tetramer." The N-terminus of a Tyr_{11}-enriched strand forms two hydrogen bonds with the N-terminus of a pure Trp_{11} strand in an adjacent symmetry-related dimer (Fig. 4). If comparable hydrogen bonds occur in solution, then they could complicate efforts to distinguish among different aggregate forms of gramicidin.

The entirely unexpected detection of a heterodimer of gramicidin in the solid state raises interesting implications concerning molecular association in a well-defined and relatively simple system. The obvious stability of the heterodimer raises the question of the relative stabilities of all gramicidin heterodimers and homodimers. The relative population of the antiparallel β-helical coils in solution may depend upon the relative stability of the different antiparallel β-ribbon precursors as well as the helices themselves.

Trp_{11}, Tyr_{11}, and β-ribbon formation and coiling

Of the residues that make up the D-L-pentadecapeptide; Val, Tyr, Trp, and Gly are more commonly observed in β-sheets than in α-helices. Only Ala, and to some extent Leu, are more frequently found in α-helices than β-sheets. This could lead to preferential formation of the β-ribbons joining

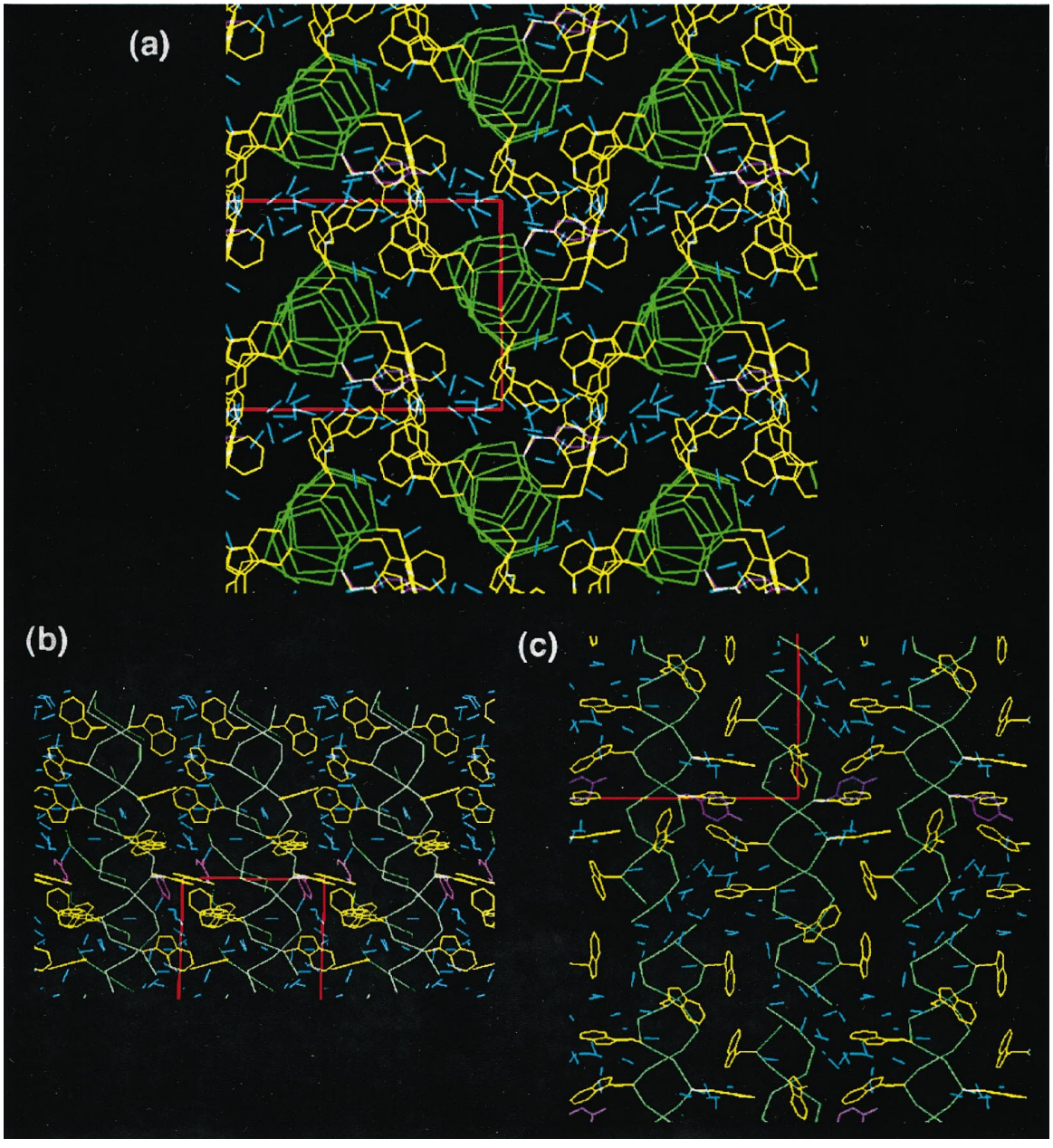

FIGURE 6 Detailed views of solvent/gramicidin interaction in the methanol-solvated crystal. (*a*) Looking down the α-axis of the crystal, the Trp planes overlap with each other and solvent fills the interstitial spaces. (*b*) Down the β-axis, the gramicidin dimers orient in pseudo-layers that are one-half unit cell thick. The methanol molecules are hydrogen-bonded to Trp side chains at the ends of the dimers. (*c*) This clustering is demonstrated further when looking perpendicular to both (*a*) and (*b*). The most solvated Trp side chains are those that lie near the dimer-dimer interface in adjacent chains.

the antiparallel strands from Val_6 through Leu_{14} with a dozen hydrogen bonds that are common to the crystallographically observed uncomplexed and cesium-complexed forms of gramicidin (Fig. 9). The ratio of occurrence of the Tyr residue in β-secondary structures versus α-secondary structures in proteins of known three-dimensional structure is significantly higher than the corresponding ratio for Trp residues (1.79 vs. 1.20) (Chou and Fasman, 1974; Lewis et al., 1971; Crawford et al., 1973). Consistent with this empirical observation, antiparallel β-ribbons incorporating gramicidin C in which a Tyr replaces a Trp may have a sufficient increase in stability to favor the formation of heterodimer β-ribbons. The absence of evidence for gramicidin C homodimers in the crystals may be controlled by mass action because the opportunities for β-strands of gramicidin C to pair with strands of gramicidin A are greater than opportunities to pair with other gramicidin C strands. Furthermore, the presence of Tyr in a hetero two-stranded β-ribbon may have enhanced potential for coil formation. The unusual pattern in ϕ ψ, χ_1, and χ_2 parameters observed for the Trp and Tyr residues in the heterodimers (Fig. 7, *a* and *b*) offers a possible explanation for

TABLE 4 ϕ, ψ Values for all residues in the three crystallized forms of gramicidin

	Methanol		Ethanol		Propanol	
	ϕ	ψ	ϕ	ψ	ϕ	ψ
Y Strand						
Val_1	−140	135	−137	145	−132	142
Gly_2	73	−154	65	−139	67	−143
Ala_3	−136	135	−152	138	−150	129
Leu_4	70	−136	92	−139	105	−139
Ala_5	−159	142	−161	88	−160	87
Val_6	94	−133	109	−150	108	−150
Val_7	−154	118	−140	129	−140	129
Val_8	89	−129	89	−128	89	−127
Trp_9	−157	126	−158	103	−160	106
Leu_{10}	93	−134	105	−143	114	−142
Tyr/Trp_{11}	−157	106	−139	111	−151	99
Leu_{12}	122	−140	101	−135	116	−142
Trp_{13}	−167	99	−158	85	−158	87
Leu_{14}	116	−146	136	−143	133	−144
Trp_{15}	−154	100	−158	83	−157	78
W Strand						
Val_1	−136	130	−158	143	−162	142
Gly_2	70	−138	65	−147	66	−146
Ala_3	−151	151	−140	126	−138	141
Leu_4	66	−139	103	−140	76	−141
Ala_5	−154	126	−157	87	−153	107
Val_6	118	−149	119	−155	104	−155
Val_7	−159	98	−140	109	−139	105
Val_8	115	−141	117	−144	120	−147
Trp_9	−157	107	−159	97	−154	102
Leu_{10}	118	−129	102	−134	100	−137
Trp_{11}	−167	98	−155	126	−154	125
Leu_{12}	120	−134	97	−129	95	−129
Trp_{13}	−160	110	−161	88	−160	89
Leu_{14}	106	−130	121	−141	120	−141
Trp_{15}	−158	81	−156	98	−159	95

the enhanced preference for β-structures of Tyr over Trp residues and the enriched presence of Tyr in double-stranded β-helical gramicidin. The ϕ, ψ plot reveals that the observed ϕ, ψ values for Trp residues in the gramicidin antiparallel β-helices are not on the optimal portion of the ϕ, ψ plot (Fig. 7 *a*) and are energetically strained to some degree. The ϕ, ψ values of Trp/Tyr residues at 11 appear less strained than the ϕ, ψ values of Trp resides at that position. On the χ_1 and χ_2 plot the conformations of the Trp's having the less common and more strained ϕ, ψ values are seen to have χ_1, χ_2 values that are more typical and exhibit correlated variations (Fig. 7 *b*). In contrast, the Trp's at position 11 have χ_1 and χ_2 values that are distinct from the more populated and well-behaved region. It may be that the stereofit of the two-stranded β-coil introduces strain that is released by distortion of the ϕ, ψ values at positions 9, 13, and 15 while permitting retention of the most favored side chain conformation with χ_1, χ_2 values around 190° and 270°, respectively.

The conformational behavior of the Trp_{11} is significantly different from that of Trp's at the 9, 13, and 15 positions. All Trp's at position 11 and both of the Tyr's at 11 take up conformations distinct from the values seen in 9/13 Trp conformations observed for residues 9, 13, and 15. It would appear that the steric crowding at the 11 position is such that a conformation in which χ_1 and χ_2 are near −160° and −90°, respectively, is incompatible with the antiparallel β-coil. Three of the Trp 11 residues have χ_1 values near −160° but the χ_2 values are near 0°; the other two Trp residues have χ_2 values of +60° and −60°. Because the side chain of Tyr is smaller than that of Trp it can adopt conformations comparable to those exhibited by Trp_{11} ($\chi_1 = -80°$, $\chi_2 = -60°$, $\chi_1 = 180°$, $\chi_2 = 60°$), but with less strain induced in the ϕ, ψ values (Fig. 7). Heterogeneous two-stranded antiparallel β-ribbons composed of one gramicidin A and one gramicidin C strand may be more stable because the Tyr size and conformation preference is more compatible with the β-ribbon structure than the Trp in the conformationally sensitive 11 position.

The ion conductance, channel duration, and selectivity of gramicidin A analogs having various combinations of Trp (W) and Phe (F) residues at positions 9, 11, 13, and 15 have been tested (Becker et al., 1991). These data demonstrate a significant influence of the substituent in the 11 position upon duration of channel opening. For the 9/16 possible W/F combinations reported, channel conductance decreases as a monotonic function of the number of W → F substitutions at the 9, 11, and 15 positions. The average duration of ion channels formed by the nine analogs studied fall into three classes. Five have an average duration similar to that of gramicidin A (850 ms), three have an average duration two to three times longer than gramicidin A (2200 ms), and one had a duration of only 5 ms. On the basis of the sample, the variation in duration appears to be highly correlated with the substituent at the 11 position. Only analogs with an 11-Phe exhibited longer duration and the one analog having the anomalous short duration had Phe in all but the 11 position (F9, W11, F13, F15). If the anomalous pattern of Trp_{11} conformation observed in the uncomplexed structure were to be present in the complexed form of gramicidin as well, the Trp_{11} side chain would shield the carbonyl oxygen of Leu^{10} as reported (Roux and Woolf, 1997), contribute to its enhanced electronegativity, and could account for evidence that there is an ion binding site inside the channel near the 11 position.

It is postulated that head-to-head dimers form when single helical monomers enter the membrane from either side of the channel, N-terminus first, and the N-termini of two such monomers find each other at the center of the bilayer to form the channel. This model raises the question of how an antibiotic peptide like gramicidin gets into the cell in the first place. A paper often cited to support this model (O'Connell et al., 1990) notes that when different analogs are added asymmetrically to opposite sides of a preformed bilayer, homodimers form in the first few minutes and that homodimer concentration remains stable while heterodimers form in increasing numbers and become the dominant form after the first few minutes. The initial dominance of homodimers indicates that although the components are added asymmetrically, each is able to migrate

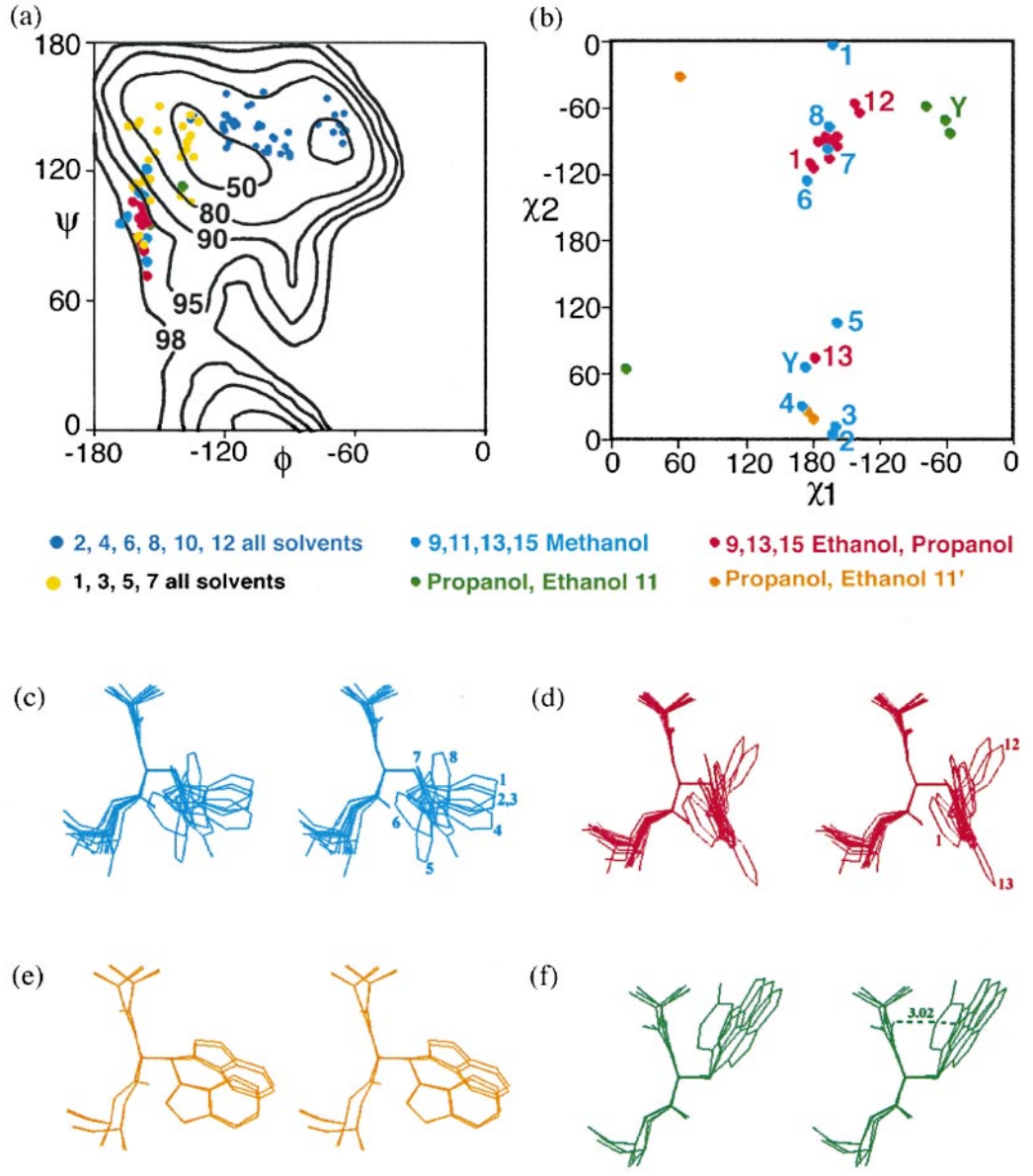

FIGURE 7 (*a*) A plot of the ϕ, ψ values for all amino acids in the six crystallographically independent strands of gramicidin in the methanol, ethanol, and n-propanol crystal forms superimposed on the contour map for amino acid conformation in high resolution structures contained in the PDB (Kleigwegt and Jones, 1996). Further reference to residues: note 9, 11, 13, and 15 are the tryptophan residues. The outer contour level encloses 98% of all non-glycine residues. Subsequent contour levels are for 95%, 90%, 80%, and 50% of all non-glycine residues. In the plot, the geometry of D-residues has been transformed to correspond to L-geometry by taking the negative of the ϕ and ϕ values. The geometries of all of the D-residues, the L-Val_1 residue, and the L-Ala_3 residues are within the 80% contour. In contrast, many of the 24 tryptophan residues have conformations outside the 95% contour. (*b*) The conformations of Trp residues at position 11 differ significantly in the χ_1 and χ_2 parameters from Trp's at positions 9, 13, and 15. All 19 Trp's at positions 9, 13, and 15 in the three different crystal forms (including one twofold disordered Trp_{13}) have χ_1 values $\approx 180°$, and 14 of these have χ_2 values near $-90°$. In contrast, the eight Trp residues at position 11 (including two twofold disorder Trp_{11}'s on a W strand (see text) in the ethanol complex and on the analogous strand in the n-propanol complex) exhibit a different pattern. The four Trp_{11}'s that have χ_1 values near 180° have χ_2 values near 0°, and the remaining four have χ_1 values closer to $\pm 60°$ than 180°. The partial-occupancy Tyr residues at position 11 have χ_1 and χ_2 values similar to those of the Trp at 11. Stereo pairs illustrate the solvent and site-specific patterns in Trp conformation, (*c*) Trp residues at positions 9, 11, 13, and 15 in gramicidin crystals grown from methanol, (*d*) Trp residues at positions 9, 13, and 15 in the crystals grown from ethanol and propanol, (*e*) conformation of Trp 11 on W strands in the heterodimer found in crystals grown from ethanol and the analogous strand in the isomorphous crystals grown from propanol, and (*f*) conformation of Trp_{11} in the Y strand in the heterodimer in crystals grown from ethanol and the analogous strand in the propanol-grown crystal. The conformations of the two partial-occupancy Tyr residues are shown in (*c*) and (*f*). The close approach of the plane of the aromatic group and the O11 backbone carbonyl is illustrated in (*f*). A consistent color scheme is used in the graphs and stereo pairs.

through the bilayer in order that the dimers that dominate ion transport in channels can proliferate. It has been postulated that these initial homodimer channels could originate from the left-handed antiparallel double-helical form because their insertion into the bilayer would be energetically favored over the insertion of the head-to-head single-helical

TABLE 5 Tryptophan (W) and tyrosine (Y) conformations

	χ_1			χ_2		
Residue	Ethanol	Propanol	Methanol	Ethanol	Propanol	Methanol
9	180	177	170	−114	−110	30
11	−57W	−62W	−160W	−83W	−77W	12W
	−79Y	13	173Y	−58Y	65	66Y
13	−139	−142	−166	−64	−55	−77
15	−166	−166	−158	−105	−106	106
29	−158	−164	−163	−94	−91	−3
31	180	175	−162	18	26	5
	61			−32		
33	−159	−176	174	−86	−90	−125
	−178			74		
35	−168	−169	−167	−86	−89	−97

dimer models. Recent NMR (Cotten et al., 1997) and HPLC (Salom et al., 1995) analysis indicate that gramicidin analogs having phenylalanine at positions 9, 11, 13, and 15 (gM) retain the left-handed antiparallel double-helical form in lipid bilayers and are poor ion conductors.

Linear gramicidin is synthesized nonribosomally by *B. brevis* (Lipmann, 1973). Infidelities in synthesis of polypeptides by polymerase enzymes occur primarily at aromatic amino acid sites. Other classes of amino acids are not generally replaced in the synthetic system, with the exception of Val_1 in linear gramicidin. Experiments to introduce unnatural amino acids have much lower rates of incorporation into growing antibiotics, unless the amino acid is present in high concentrations (Lipmann, 1973). One could ask why amino acid heterogeneity does not occur at Trp_9, Trp_{13}, and Trp_{15}, but does occur at Trp_{11}. It may be that infidelity observed in gramicidin D synthesis is not random, but that a selective evolutionary advantage to *B. brevis* is provided by heterogeneity at positions 1 and 11. Molecular features observed in crystals of gramicidin from methanol and ethanol suggest a role for this natural heterogeneity. Both structures contain a minor, but significant (20–30%), fraction of Tyr_{11} instead of Trp_{11} that would have evolutionary advantage. This heterogeneity occurs on only one of the two strands in the dimer, therefore forming a heterodimer. It is obvious that heterodimers of linear gramicidin are a significant chemical species in mixtures of gramicidin. The Tyr_{11} on gramicidin C may be critically important to stabilization of the antiparallel β-ribbon and its conversion to the β-helix to create a template for formation of homodimers of gramicidin A via specific end-to-end hydrogen bonds (Fig. 4). It is also possible that this heterogeneity may play a role in one of the other postulated functions of gramicidin.

In addition to stabilizing the antiparallel β-ribbon the Tyr residue plays a critical role in determining the aggregation of dimers in the two crystal forms. Despite efforts to crystallize hundreds of samples of natural and synthetic gramicidins, the only crystals for which x-ray crystal structure analysis has been reported have been prepared from gramicidin samples containing natural abundance gA/gB/gC. If it were not for the high resolution data provided by the well-formed crystals of uncomplexed gramicidin, the presence of Tyr_{11} in the heterodimers would have gone undetected. It remains to be seen whether the presence of some minimal percentage of gC is necessary and sufficient for crystallization. If, as these data suggest, a small percentage of gC acts as a nucleation agent for crystallization of gA, it is conceivable that a similar phenomenon may account for anomalous protein and peptide aggregation in other systems. The possibility that a minor component in a heterogeneous mixture

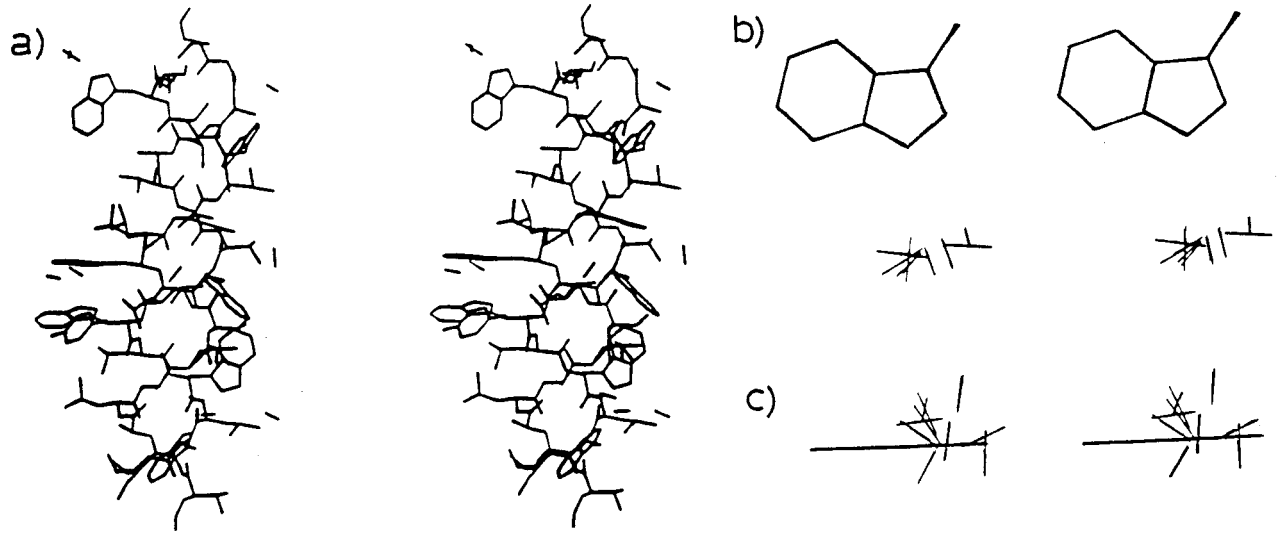

FIGURE 8 (*a*) The structure of methanol-solvated gramicidin D shows little or no influence of crystal packing upon solvent association. The positions of the 10 methanol molecules that are hydrogen-bonded to 10 indole rings are seen to be nearly identical relative to the Trp plan and are governed by the conformation of the tryptophan residues, not crystal packing; a superposition of the position of 10 methanol molecules is viewed perpendicular to the indole ring in (*b*) and parallel to the indole ring in (*c*). This gramicidin conformation including the Trp orientations and associated solvent probably constitutes the major conformer present in polar solvents.

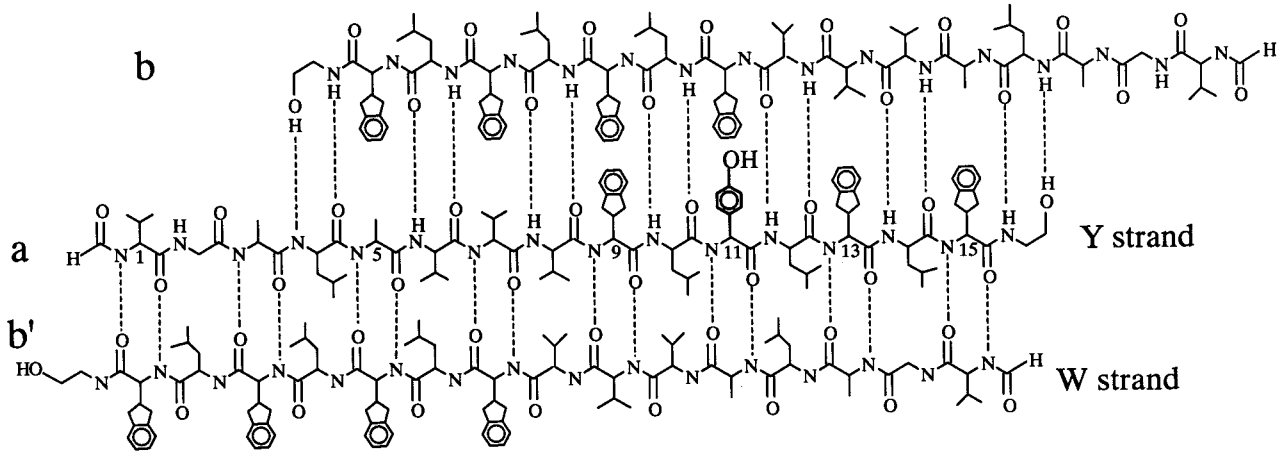

FIGURE 9 The two sets of hydrogen bonds that unite the antiparallel β strands of the $\beta^{5.6}$ helical dimer differ significantly. One set of 16 hydrogen bonds between (*a*) and (*b′*) are all N–H–O hydrogen bonds typical of a β-sheet. The 14 hydrogen bonds between (*a*) and (*b′*) include two O–H–N hydrogen bonds contributed by the ethanolamine hydroxyl. The set of 14 hydrogen bonds is retained in the CsCl complex, suggesting that the simplest transition between the open and closed pore could involve rearrangement of the hydrogen bond strand by a four-residue shift in the inter-β strand hydrogen bonding.

can have a profound effect on peptide folding and aggregation has potential applications to other systems in which anomalous behavior is exhibited by aggregation of apparently homogeneous materials, such as the enigmatic behavior of the prion, responsible for bovine spongiform encephalitis and ovine scrapie, as well as the human equivalents, kuru, Creutzfeldt-Jakob disease, and Gerstmann-Straussler syndrome. These diseases have been linked to a template-driven protein conformational change requiring the presence of small amounts of PrP^{Sc}, a conformational mutant of a naturally occurring protein PrP^{C}, that forms heterodimers as a part of the disease process (Cohen et al., 1994).

This work was supported by National Institutes of Health/NIGMS Grant GM32812.

REFERENCES

Arseniev, A. S., I. L. Barsukov, A. L. Lomize, V. Y. Orekhov, and V. F. Bystrov. 1992. Refinement of the spatial structure of the gramicidin A transmembrane ion-channel. *(Russian), Biol. Membr. (USSR).* 18:182.

Becker, M. D., D. V. Greathouse, R. E. Koeppe II, and O. S. Andersen. 1991. Amino acid sequence modulation of gramicidin channel function: effects of tryptophan-to-phenylalanine substitutions on the single-channel conductance and curation. *Biochemistry.* 30:8830–8839.

Bernstein, F. C., T. F. Koetzle, G. J. Williams, E. F. Meyer, M. D. Brice, J. B. Rogers, O. Kennard, T. Shimanouchi, and M. Tasuni. 1977. The Protein Data Bank: a computer-based archival file for macromolecular structures. *J. Mol. Biol*. 112:535–542.

Bouchard, M., J. H. Davis, and M. Auger. 1995. High-speed magic angle spinning solid-state ^{1}H nuclear magnetic resonance study of the conformation of gramicidin A in lipid bilayers. *Biophys. J.* 69:1933–1938.

Brunger, A. T. 1992. Free R value: a novel statistical quantity for assessing the accuracy of crystal structures. *Nature.* 355:472–474.

Chou, P. Y., and G. D. Fasman. 1974. Conformational parameters for amino acids in helical, β-sheet, and random coil regions calculated from proteins. *Biochemistry*. 13:211. Prediction of protein conformation, ibid., p. 222.

Cohen F. E., K. M. Pan, Z. Huang, M. Baldwin, R. J. Fletterick, and S. B. Prusiner. 1994. Structural clues to prion replication. *Science.* 264: 530–531.

Cotten, M., Feng Xu, and T. A. Cross. 1997. Protein stability and conformational rearrangements in lipid bilayers: linear gramicidin, a model system. *Biophys. J.* 73:614–623.

Crawford, J. L., N. N. Lipscomb, and C. G. Schellman. 1973. The reverse turn as a polypeptide conformation in globularproteins. *Proc. Natl. Acad. Sci. USA.* 70:538–542.

CRC Handbook of Chemistry & Physics. 1976. 56th ed. CRC Press, Cleveland, OH. E-58.

Doyle, D. A., and B. A. Wallace. 1997. Crystal structure of the gramicidin/potassium thiocyanate complex. *J. Mol. Biol.* 266:963–977.

Dubos, R. J. 1939. Studies on a bactericidal agent extracted from a soil bacillus. *J. Exp. Med.* 70:1–10.

Durkin, J. T., O. S. Anderson, E. R. Blout, F. Heitz, R. E. Koeppe, and Y. Trudelle. 1986. Structural information from functional measurements. Single channel studies of gramicidin analogs. *Biophys. J.* 49:118–121.

Gross, E., and B. Witkop. 1965. Gramicidin. IX. Preparation of gramicidin A, B, and C. *Biochemistry.* 4:2495–2501.

Hotchkiss, R. D. 1944. Gramicidin, tyrocidine, and tyrothricin. *Adv. Enzymol.* 4:153–199.

Jing, N., and D. W. Urry. 1995. Ion pair binding of Ca^{2+} and Cl^{-} ions in micellar-packaged gramicidin A. *Biochim. Biophys. Acta.* 1238:12–21.

Ketchem, R. R., W. Hu, and T. A. Cross. 1993. High-resolution conformation of gramicidin A in a lipid bilayer by solid-state NMR. *Science*. 261:1457–1460.

Kleigwegt, G. J., and T. A. Jones. 1996. Phi/psi-chology: Ramachandran revisited. *Structure.* 4:1395.

Koeppe II, R. E., D. V. Greathouse, L. L. Providence, and O. S. Anderson. 1991. [L-Leu 9-D-Trp 10-L-Leu 11-D-Trp 12-L-Leu l3-D-Trp l4-L-Leu 15]-gramicidin forms both single- and double-helical channels. *Biophys. J.* 59:319*a*. (Abstr.).

Koeppe II, R. E., J. A. Paczkowski, and W. L. Whaley. 1985. Gramicidin K, a new linear channel-forming gramicidin from *Bacillus brevis. Biochemistry*. 24:2822–2826.

Koeppe II, R. E., J. A. Killian, T. C. Vogt, B. de Kruijff, M. J. Taylor, G. L. Mattice, and D. V. Greathouse. 1995. Palmitoylation-induced conformational changes of specific side chains in the gramicidin transmembrane channel. *Biochemistry.* 34:9299–9306.

Koeppe II, R. E., L. L. Providence, D. V. Greathouse, F. Heitz, Y. Trudelle, N. Purdie, and O. D. Andersen. 1992. On the helix sense of gramicidin A single channels. *Proteins Struct., Funct., Genet.* 12:49–62.

Langs, D. A. 1988. Three-dimensional structure at 0.86 Å of the uncomplexed form of the transmembrane ion channel peptide gramicidin A. *Science.* 241:188–191.

Langs, D. A., G. D. Smith, C. Courseille, G. Précigoux, and M. Hospital. 1991. The monoclinic uncomplexed $\uparrow \downarrow \beta^{5.6}$ form of gramicidin A:

alternate patterns of helical association with membrane bilayers. *Proc. Natl. Acad. Sci.USA.* 88:5345–5349.

Lewis, P. N., F. A. Momany, and H. S. Scheraga. 1971. Folding of polypeptide chains in proteins: a proposed mechanism for folding. *Proc. Natl. Acad. Sci. USA.* 68:2293.

Lipmann, F. 1973. Nonribosomal polypeptide synthesis on polyenzyme templates. *Acc. Chem. Res.* 6:361–367.

Nekrasov, A. N., A. V. Stepanov, and V. P. Timofeev. 1995. The features of the spatial structure of the gramicidin A-cesium complex. *FEBS Lett.* 371:35–38.

O'Connell, A. M., R. E. Koeppe II, and O. S. Andersen. 1990. Kinetics of gramicidin channel formation in lipid bilayers: transmembrane monomer association. *Science.* 250:1256–1259.

Oiki, S., R. E. Koeppe II, and O. S. Andersen. 1994. Asymmetric gramicidin channels: heterodimeric channels with a single F_6Val^1 residue. *Biophys. J.* 66:1823–1832.

Pascal, S. M., and T. A. Cross. 1993. High-resolution structure and dynamic implications for a double-helical gramicidin A conformer. *J. Biomol. NMR.* 3:495–513.

Pressman, B. C. 1965. Induced active transport of ions in mitochondria. *Proc. Natl. Acad. Sci. USA.* 53:1076–1083.

Roux, B., B. Prod'hom, and M. Karplus. 1995. Ion transport in the gramicidin channel: molecular dynamics study of single and double occupancy. *Biophys. J.* 68:876–892.

Roux, B., and T. B. Woolf. 1997. The binding site of sodium in the gramicidin channel. Comparison of molecular dynamics and solid-state nMR data. 41st Annual Meeting of the Biophysical Society, New Orleans, Louisiana.

Sack, J. S. 1988. CHAIN—A crystallographic modeling program. *J. Mol. Graphics.* 6:224–225.

Salom, D., M. C. Bañò, L. Braco, and C. Abad. 1995. HPLC demonstration that an all Trp→Phe replacement in gramicidin A results in a conformational rearrangement from β-helical monomer to double-stranded dimer in model membranes. *Biochem. Biophys. Res. Commun.* 209: 466–473.

Sarges, R., and B. Witkop. 1965. The structure of valine and isoleucine-gramicidin A. *J. Am. Chem. Soc.* 87:2011–2020.

Sawyer, D. B., R. E. Koeppe II, and O. S. Andersen. 1989. Induction of conductance heterogeneity in gramicidin channels. *Biochemistry.* 28: 6571–6583.

Seoh, S.-A., and D. Busath. 1995. Gramicidin tryptophans mediate formamidinium-induced channel stabilization. *Biophys. J.* 68:2271–2279.

Separovic, F., J. Gehrmann, T. Milne, B. A. Cornell, S. Y. Lin, and R. Smith. 1994. Sodium ion binding in the gramicidin A channel. Solid-state NMR studies of the tryptophan residues. *Biophys. J.* 67:1495–1500.

Sheldrick, G. M. 1997. SHELXL-97: A Program for the Refinement of Crystal Structures. Univ. of Göttingen, Germany.

Smith, R., D. E. Thomas, A. R. Atkins, F. Separovic, and B. A. Cornell. 1990. Solid-state ^{13}C-NMR studies of the effects of sodium ions on the gramicidin A ion channel. *Biochim. Biophys. Acta.* 1026:161–166.

Stark, G., M. Strässle, and Z. Takacz. 1986. Temperature-jump and voltage-jump experiments at planar lipid membranes support an aggregational (micellar) model of the gramicidin A ion channel. *J. Membr. Biol.* 89:23–37.

Takeuchi, H., Y. Nemoto, and I. Harada. 1990. Environments and conformations of tryptophan side chains of gramicidin A in phospholipid bilayers studied by Raman spectroscopy. *Biochemistry.* 29:1572–1579.

Urry, D. W. 1971. The gramicidin A transmembrane channel: A proposed $\mathfrak{z}_{LD}$ helix. *Proc. Natl. Acad. Sci. USA.* 68:672–676.

Urry, D. W., K. U. Prasad, and T. L. Trapane. 1982a. Location of monovalent cation binding sites in gramicidin channel. *Proc. Natl. Acad. Sci. USA.* 79:390–394.

Urry, D. W., J. T. Walker, and T. L. Trapane. 1982b. Ion interactions in (1-^{13}C)D-Val^8 and D-Leu^{14} analogs of gramicidin A, the helix sense of the channel and location of ion binding sites. *J. Membr. Biol.* 69: 225–231.

Veatch, W., and L. Stryer. 1977. The dimeric nature of the gramicidin A transmembrane channel: conductance and fluorescence energy transfer studies of hybrid channels. *J. Mol. Biol.* 113:89–192.

Wallace, B. A., and K. Ravikumar. 1988. The gramicidin pore: crystal structure of a cesium complex. *Science.* 241:182–187.

Woolf, T. B., and B. Roux. 1997. The binding site of sodium in the gramicidin A channel: comparison of molecular dynamics with solid-state NMR data. *Biophys. J.* 72:1930–1945.

Zhang, Z., S. M. Pascal, and T. A. Cross. 1992. A conformational rearrangement in gramicidin A: from a double-stranded left-handed to a single-stranded right-handed helix. *Biochemistry.* 31:8822–8828.